

*Supporting information for*

# Palladium Nanoparticles Supported on Surface-Modified Metal Oxides for Catalytic Oxidation of Lean Methane

Cunshuo Li<sup>a</sup>, Wenzhi Li<sup>a\*</sup>, Kun Chen<sup>a</sup>, Ajibola T. Ogunbiyi<sup>a</sup>, Zean Zhou<sup>a\*</sup>, Fengyang Xue<sup>a</sup>,  
and Liang Yuan<sup>b</sup>

a. Laboratory of Basic Research in Biomass Conversion and Utilization, Department of  
Thermal Science and Energy Engineering, University of Science and Technology of China,  
Hefei 230026, China

b. National & Local Joint Engineering Research Center of Precision Coal Mining, Anhui  
University of Science and Technology, Huainan, 232001, China

## **Corresponding Author**

\*Wenzhi Li

Email: liwenzhi@ustc.edu.cn

\*Zean Zhou

Email: zhouzean@ustc.edu.cn

## METHODS

**Preparation of palladium catalysts supported on surface-modified metal oxides** 3 g of support powder and 1.65 mL triethoxy(octyl)silane (TEOOS, 97%) were first dispersed in 60 mL toluene by sonication for 20 min. Under vigorous stirring, the resultant mixture was refluxed at 110 °C for 3 h, then collected by centrifugation (6000 rpm for 3 min) and washed abundantly with toluene. Finally, the hydrophobic supports were obtained by drying under -0.09 MPa vacuum and stored as support materials for palladium catalysts.

Supported palladium catalysts were prepared by wetness impregnation method. For catalysts with a nominal Pd content of 1.0 wt%, 5.3 mL of palladium acetate solution (2 mg/mL, dissolved in toluene) was first stirred with 500 mg of hydrophobic support powder for 10 min, then the mixture was sonicated for another 30 min and dried at 70 °C under vacuum for 8 h before the final calcination (500 °C for 3 h).

**Characterization of catalysts** Ion-coupled plasma atomic emission spectroscopy was performed to ensure the actual loading of Pd by a Optima 7300DV (PerkinElmer Co., USA). Before CO chemisorption (chemstar TPx chemisorption instrument, Quantachrome Co., USA), the samples were reduced in 10% H<sub>2</sub>/Ar at 300 °C for 1 h, and the volume of pulse loop was calibrated to be 516 μL. Nitrogen-physisorption was operated at ~77K on a Micromeritics Tristar III 3020 instrument to obtain the BET surface areas of discussed samples. Samples X-ray diffraction (XRD) patterns were obtained with a Rigaku TTR-III diffractor using Cu K<sub>α</sub> radiation (40 kV, 200 mA). The diffraction spectra were recorded in

the  $2\theta$  range of 20 to 80° with a scanning step of 0.02°. Scanning electron microscopy (SEM, FEI XL-30 ESEM) and field-emission transmission electron microscope (FETEM JEOL-JSM-2100F instrument) were performed to depict the morphology of selected samples, and the lattice fringe spacing was measured at high-resolution mode. The high-resolution elemental mapping of HfO<sub>2</sub>-supported palladium catalysts were obtained by Talos F200X (FEI Electron optics Co., USA) coupled with energy dispersive X-ray spectroscopy (EDX). X-ray photoelectron spectroscopy (XPS) analysis was taken on a Thermo ESCALAB 250 spectrometer system with Al K<sub>α</sub> x-ray source (1486.6 eV) at ultrahigh vacuum. The XPS spectra were deconvoluted with the XPSPEAK 4.1 software and calibrated against the C1s line (284.8 eV) originating from adventitious carbon. Hydrogen-temperature programmed reduction (H<sub>2</sub>-TPR) and oxygen-temperature desorption (O<sub>2</sub>-TPD) was taken with a chemstar TPx chemisorption instrument (Quantachrome Co., USA). The signals caused by H<sub>2</sub> consumption and O<sub>2</sub> desorption were detected by a TCD detector. In situ diffuse reflectance infrared (DRIFT) was recorded on a Niolet iS50 FTIR spectrometer equipped with a MCT detector and an elevated-temperature reaction chamber. Catalyst samples were placed in the reaction chamber and pretreated with reactant gas (1.0 vol% CH<sub>4</sub>, air as balance) at a rate of 20 mL/min at 500°C for 1h, then DRIFT spectra were recorded at temperatures of 150, 200, 250, 300, 350, 400, 450 and 500°C under gas flow after cooling down to room temperature. The spectrum of each catalyst sample at a particular temperature was the accumulation of 32 scans with a resolution of 4 cm<sup>-1</sup>.

**Performance evaluation of catalysts** The catalytic combustion of lean methane was conducted in a fixed-bed quartz reactor with an internal diameter of 3.0 mm at ambient

pressure. Typically, 20 mg of catalyst was fixed by quartz glass wool while the reactants (1 vol% CH<sub>4</sub> balanced with air) was fed through the sample via a mass flow controller. The flow rate of reactant gas was maintained at 20 standard-state cubic centimeter per minute (SCCM), which corresponds to a gas hourly space velocity (GHSV) of 60,000 mLg<sup>-1</sup>h<sup>-1</sup>. The effluents were monitored by an on-line GC-1690 gas chromatography equipped with a flame ionization detector (FID), and the conversion of methane was calculated according to the integral areas of residual methane. Prior to each measurement, the samples were activated in reactant gas at 500°C for 1 h.

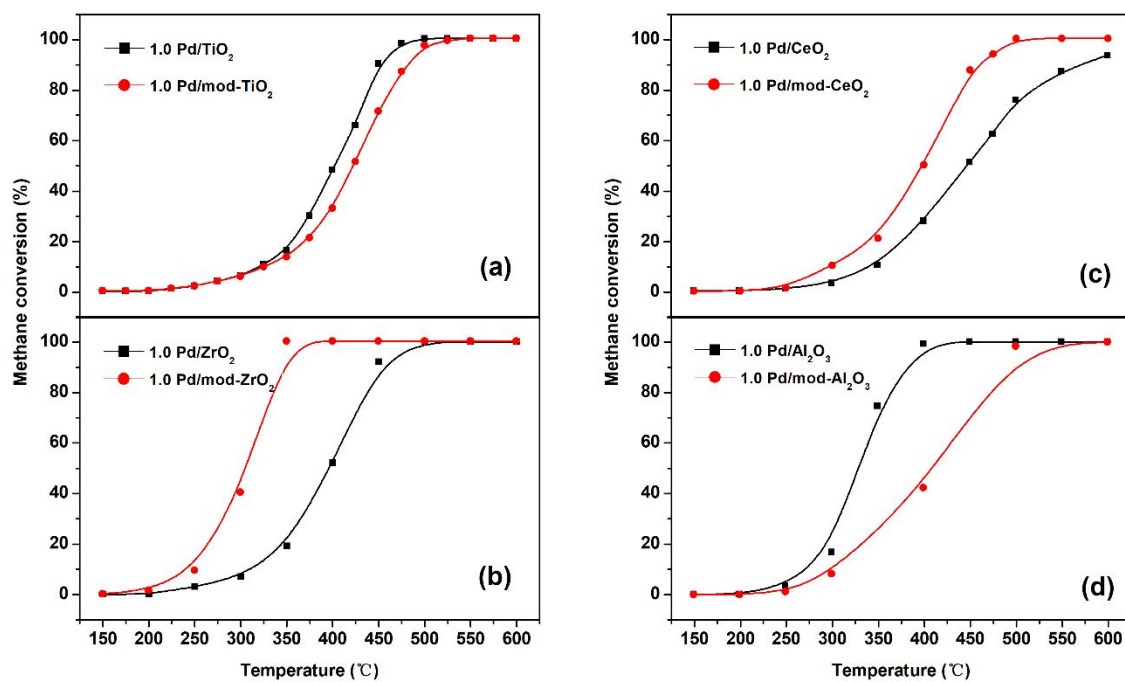


**Fig. S1.** Methane conversion as a function of temperature over (a) 1.0Pd/TiO<sub>2</sub>, 1.0Pd/mod-TiO<sub>2</sub>, (b) 1.0Pd/ZrO<sub>2</sub>, 1.0Pd/mod-ZrO<sub>2</sub>, (c) 1.0Pd/CeO<sub>2</sub>, 1.0Pd/mod-CeO<sub>2</sub> and (d) 1.0Pd/Al<sub>2</sub>O<sub>3</sub>, 1.0Pd/mod-Al<sub>2</sub>O<sub>3</sub>.

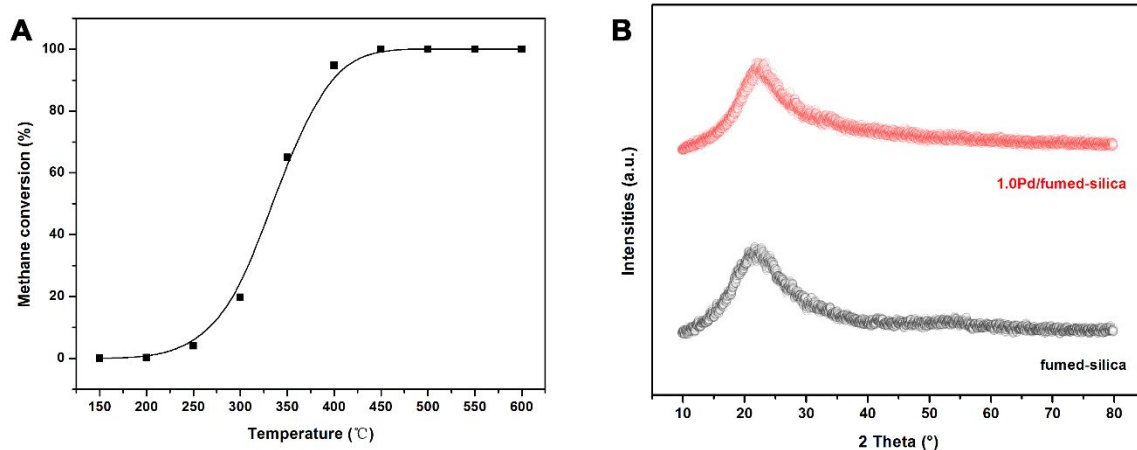


**Fig. S2.** (A) Light-off curves of 1.0Pd/fumed-silica, (B) the XRD patterns of fumed-silica and its supported palladium catalyst. The amorphous nature of fumed-silica was confirmed by its characteristic broad peak located at 22°, and the deposition of palladium did not alter its structure.

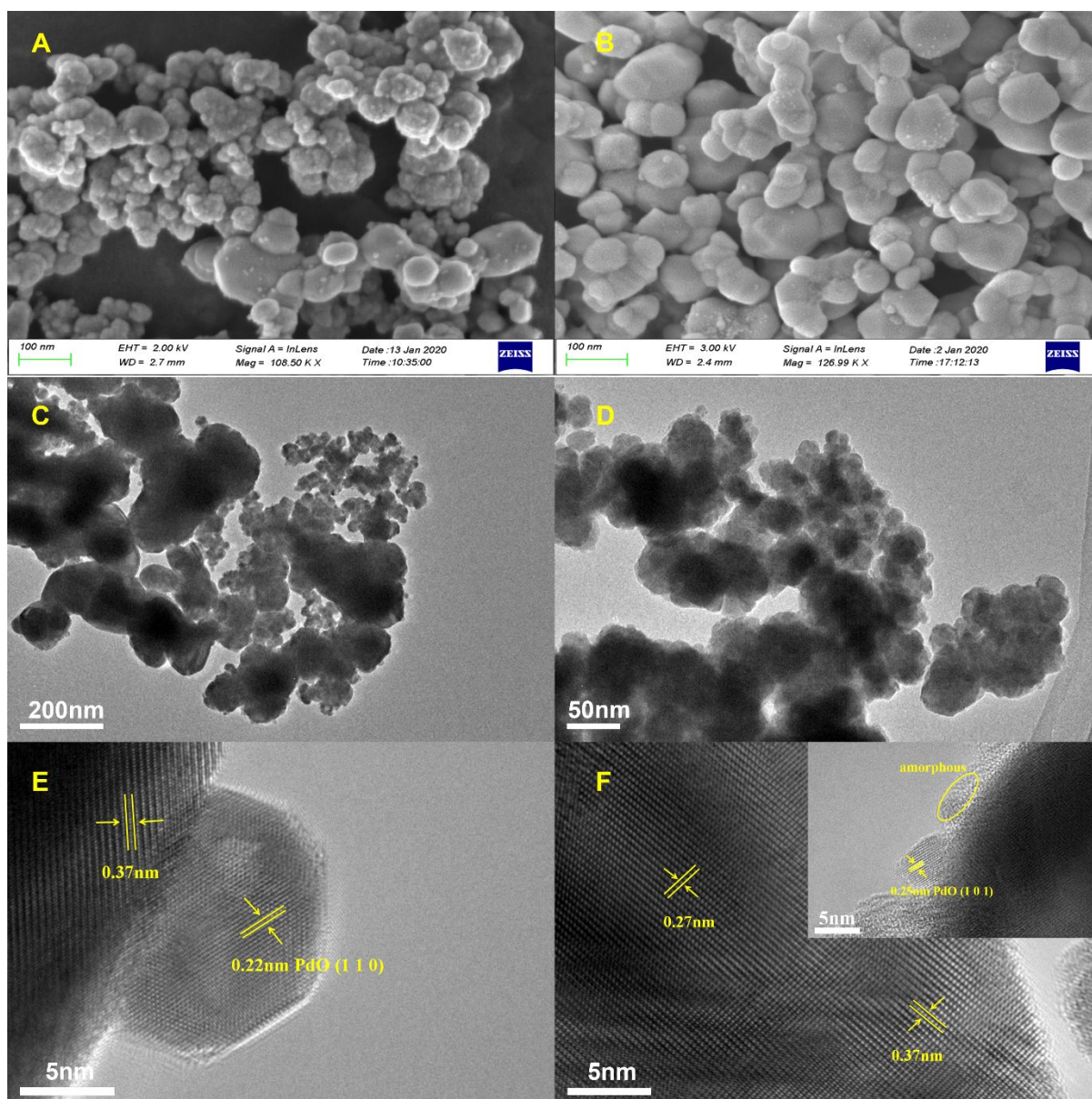


**Fig. S3.** Representative SEM, TEM and HRTEM images of (A, C, E) 1.0Pd/HfO<sub>2</sub> and (B, D, F) 1.0Pd/mod-HfO<sub>2</sub>.

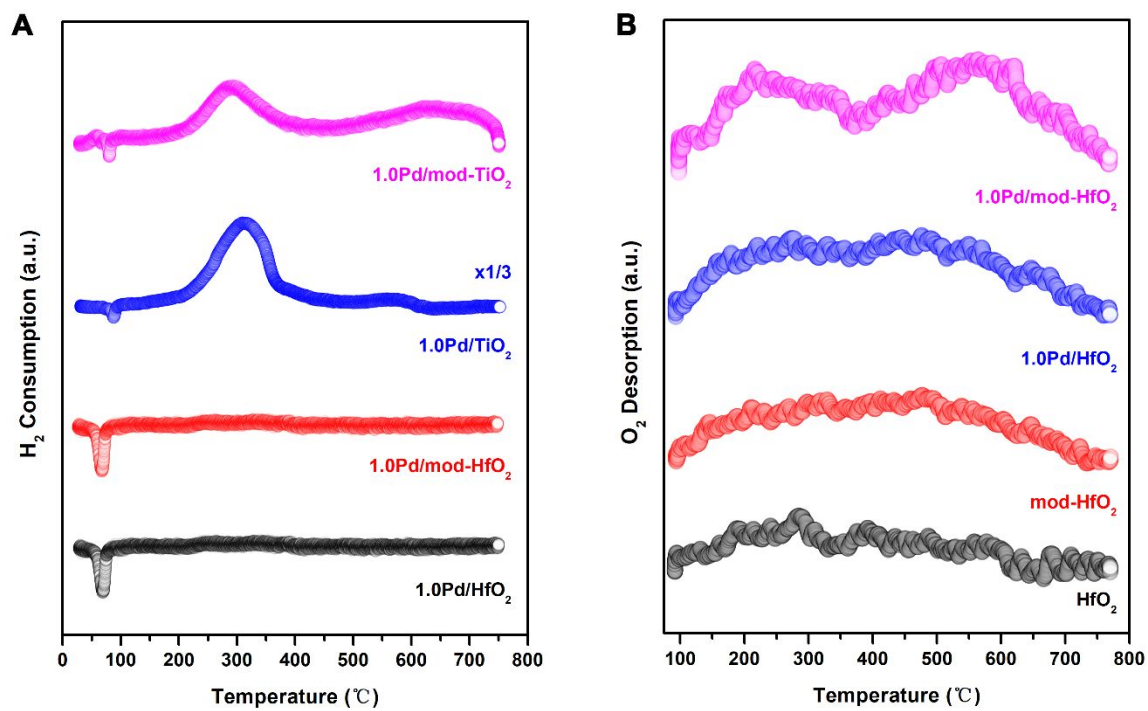


**Fig. S4.** (A) H<sub>2</sub>-TPR curves of 1.0Pd/HfO<sub>2</sub>, 1.0Pd/mod-HfO<sub>2</sub>, 1.0Pd/TiO<sub>2</sub> and 1.0Pd/mod-TiO<sub>2</sub>, and (B) O<sub>2</sub>-TPD curves of HfO<sub>2</sub>, mod-HfO<sub>2</sub>, 1.0Pd/HfO<sub>2</sub> and 1.0Pd/mod-HfO<sub>2</sub>.



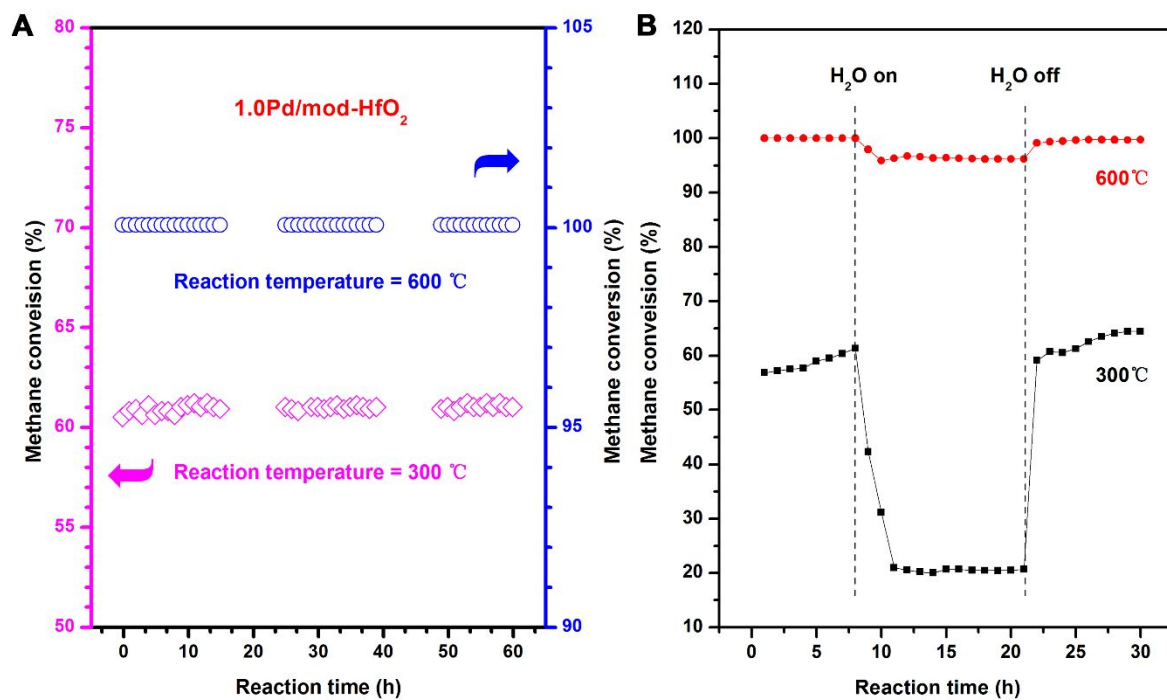


**Fig. S5.** (A) On-stream reaction over 1.0Pd/mod-HfO<sub>2</sub> at 300 °C and 600 °C, (B) effect of water introduction and removal in the feedstock over 1.0Pd/mod-HfO<sub>2</sub> at 300 °C and 600 °C (H<sub>2</sub>O concentration 5.0 vol%).

**Table S1.** Catalytic activities of samples supported on various metal oxides at GHSV=60,000 mLg<sup>-1</sup>h<sup>-1</sup>.

Catalyst	T <sub>50</sub> [°C]	Catalyst	T <sub>50</sub> [°C]
1.0Pd/TiO <sub>2</sub>	404	1.0Pd/mod-TiO <sub>2</sub>	423
1.0Pd/ZrO <sub>2</sub>	396	1.0Pd/mod-ZrO <sub>2</sub>	305
1.0Pd/CeO <sub>2</sub>	448	1.0Pd/mod-CeO <sub>2</sub>	399
1.0Pd/Al <sub>2</sub> O <sub>3</sub>	328	1.0Pd/mod-Al <sub>2</sub> O <sub>3</sub>	408

**Table S2.** A literature review of methane combustion activity over supported Pd catalysts in terms of  $T_{50}$  and  $T_{90}$ .

Catalyst	Concentration of CH <sub>4</sub> [vol%]	GHSV [mLg <sup>-1</sup> h <sup>-1</sup> ]	T <sub>50</sub> [°C]	T <sub>90</sub> [°C]	Reference
Pd/LaFeO <sub>3</sub>	1.0	18,400	460	600	1
Pd@CeO <sub>2</sub> /H-Al <sub>2</sub> O <sub>3</sub>	0.5	200,000	320	370	2
Pd/LaMnO <sub>3</sub>	1.0	20,000	425	500	3
AuPd/meso-Co <sub>3</sub> O <sub>4</sub>	2.5	20,000	280	324	4
Au Pd/3DOM LSMO	5.0	50,000	314	336	5
Pd/Co <sub>3</sub> O <sub>4</sub>	2.0	12,000	333	370	6
Pd/o-CeO <sub>2</sub>	1.0	30,000	309	348	7
Pd/m-zeolite	1.0	69,000	355	375	8
Pd/κ-CZ	1.0	30,000	305	345	9
Pd/mod-HfO <sub>2</sub>	1.0	60,000	288	317	Present work

**Table S3.** Assignment of common intermediates during methane combustion.

Intermediates	References [cm <sup>-1</sup> ]	1.0Pd/mod-HfO <sub>2</sub> [cm <sup>-1</sup> ]	1.0 Pd/HfO <sub>2</sub> [cm <sup>-1</sup> ]
Formaldehyde (CH <sub>2</sub> O)	$\omega$ (CH <sub>2</sub> ):1250+1415 <sup>5</sup>	n.a.	1245+1400
Formic acid (HCOO <sup>-</sup> )	$\nu_s$ (C-O):1340-1390 <sup>10, 11</sup> $\nu_{as}$ (C-O):1580-1590 <sup>5</sup>	1365 1580	1350 1585
Monodentate carbonate (m-CO <sub>3</sub> <sup>2-</sup> )	$\nu_s$ (C-O):1330-1370 <sup>10-12</sup> $\nu_{as}$ (C-O):1470-1530 <sup>10-12</sup>	1330 1520	1350 1530

n.a.: Not available.

## REFERENCES

1. Eyssler, A.; Winkler, A.; Mandaliev, P.; Hug, P.; Weidenkaff, A.; Ferri, D., Influence of thermally induced structural changes of 2 wt% Pd/LaFeO<sub>3</sub> on methane combustion activity. *Appl. Catal., B* **2011**, *106* (3-4), 494-502.
2. Cargnello, M.; Jaén, J. J. D.; Garrido, J. C. H.; Bakhmutsky, K.; Montini, T.; Gámez, J. J. C.; Gorte, R. J.; Fornasiero, P., Exceptional Activity for Methane Combustion over Modular Pd@CeO<sub>2</sub> Subunits on Functionalized Al<sub>2</sub>O<sub>3</sub>. *Science* **2012**, *337*, 713-717.
3. Guo, G.; Lian, K.; Gu, F.; Han, D.; Wang, Z., Three dimensionally ordered macroporous Pd-LaMnO<sub>3</sub> self-regeneration catalysts for methane combustion. *Chem. Commun.* **2014**, *50* (88), 13575.
4. Wu, Z.; Deng, J.; Liu, Y.; Xie, S.; Jiang, Y.; Zhao, X.; Yang, J.; Arandiyán, H.; Guo, G.; Dai, H., Three-dimensionally ordered mesoporous Co<sub>3</sub>O<sub>4</sub>-supported Au–Pd alloy nanoparticles: High-performance catalysts for methane combustion. *J. Catal.* **2015**, *332*, 13-24.
5. Wang, Y.; Arandiyán, H.; Scott, J.; Akia, M.; Dai, H.; Deng, J.; Kondo-Francois; Aguey-Zinsou; Amal, R., High Performance Au–Pd Supported on 3D Hybrid Strontium-Substituted Lanthanum Manganite Perovskite Catalyst for Methane combustion. *ACS Catal.* **2016**, *6*, 6935-6947.
6. Ercolino, G.; Stelmachowski, P.; Grzybek, G.; Kotarba, A.; Specchia, S., Optimization of Pd catalysts supported on Co<sub>3</sub>O<sub>4</sub> for low-temperature lean combustion of residual methane. *Appl. Catal., B* **2017**, *206*, 712-725.

7. Lei, Y.; Li, W.; Liu, Q.; Lin, Q.; Zheng, X.; Huang, Q.; Guan, S.; Wang, X.; Wang, C.; Li, F., Typical crystal face effects of different morphology ceria on the activity of Pd/CeO<sub>2</sub> catalysts for lean methane combustion. *Fuel* **2018**, *233*, 10-20.
8. Losch, P.; Huang, W.; Vozniuk, O.; Goodman, E. D.; Schmidt, W.; Cargnello, M., Modular Pd/Zeolite Composites Demonstrating the Key Role of Support Hydrophobic/Hydrophilic Character in Methane Catalytic Combustion. *ACS Catal.* **2019**, *9*, 4742-4753.
9. Ding, Y.; Wu, Q.; Lin, B.; Guo, Y.; Guo, Y.; Wang, Y.; Wang, L.; Zhan, W., Superior catalytic activity of a Pd catalyst in methane combustion by fine-tuning the phase of ceria-zirconia support. *Appl. Catal., B* **2020**, *266*, 118631.
10. Jodłowski, P. J.; Chlebda, D.; Piwowarczyk, E.; Chrzan, M.; Jędrzejczyk, R. J.; Sitarz, M.; Węgrzynowicz, A.; Kołodziej, A.; Łojewska, J., In situ and operando spectroscopic studies of sonically aided catalysts for biogas exhaust abatement. *J. Mol. Struct.* **2016**, *1126*, 132-140.
11. Jodłowski, P. J.; Jędrzejczyk, R. J.; Chlebda, D.; Gierada, M.; Łojewska, J., In situ spectroscopic studies of methane catalytic combustion over Co,Ce, and Pd mixed oxides deposited on a steel surface. *J. Catal.* **2017**, *350*, 1-12.
12. Li, J.; Liang, X.; Xu, S.; Hao, J., Catalytic performance of manganese cobalt oxides on methane combustion at low temperature. *Appl. Catal., B* **2009**, *90* (1-2), 307-312.